IEEE Open Journal of the
Industrial Electronics Society

Received 1 July 2020; revised 28 July 2020; accepted 12 August 2020. Date of publication 18 August 2020;
date of current version 4 September 2020. The review of this article was arranged by Associate Editor Francisco D. Freijedo.

Digital Object Identifier 10.1109/OJIES.2020.3017379

A Unified Method for Generic Signal Parameter Estimation of Arbitrarily Distorted Single-Phase Grids With DC-Offset

CHRISTOPH HACKL [1] (Senior Member, IEEE), AND MARKUS LANDERER [1,2]

[1] Munich University of Applied Sciences (MUAS), 80335 Munich, Germany
[2] Technical University of Munich (TUM), 85748 Garching, Germany

CORRESPONDING AUTHOR: MARKUS LANDERER (e-mail: markus.landerer@tum.de)

ABSTRACT A unified method is presented which allows to estimate dc-offset, all harmonic components *and* fundamental frequency in arbitrarily distorted single-phase grids using a *Frequency Adaptive Observer (FAO)* consisting of *modified Second-Order Generalized Integrators (mSOGIs)*, an adaptive *DC-Integrator (DCI)* and a *modified Frequency Locked Loop (mFLL)*. DCI and mSOGIs are tuned by *pole placement* which allows for an arbitrarily fast detection of dc-offset and harmonic components if the fundamental frequency is known. If the fundamental frequency must be estimated as well, an mFLL with *Gain Normalization (GN)*, *Rate Limitation (RL)*, *Anti-Windup (AW)* strategy and *low-pass filters (LPF)* must be employed. The effectiveness of the proposed FAO is validated by experimental results and its enhanced performance is shown and compared to existing estimation methods.

INDEX TERMS Dc-offset estimation, frequency adaptive observer, frequency estimation, frequency locked loop, harmonics estimation, second-order generalized integrator.

I. MOTIVATION AND LITERATURE REVIEW

In the future, as large-scale generation systems will be replaced by decentralized energy production like wind or solar, which are coupled to the grid by power electronic devices, the overall grid inertia will diminish. As a consequence, fast(er) frequency fluctuations and (more) distorted voltages and/or currents might occur endangering grid stability and voltage quality which may lead to partial blackouts, the destruction of electronic devices or a threat to human's life. In particular, the presence of dc-offsets will result in malfunctioning grid converters [1]. Additionally, distorted grid voltages and currents yield equivalently distorted electrical power flows in the grid which then possibly also contain dc-offset and harmonics with varying frequencies. To take appropriate countermeasures, firstly these distortions must be identified as fast and precise as possible to protect users from malfunctioning equipment and to prevent destruction of electronic devices. Therefore, in the recent years, much effort has been put into this research question which resulted in the development of *Second-Order Generalized Integrators (SOGIs)* [2]–[16].

These SOGIs rely on an oscillation capability, i.e. they can reduplicate any non-distorted sinusoid (and, as side product, its quadrature signal) with known and constant frequency. For proper functionality, if the frequency is unknown or varying, the SOGIs must be equipped with a *Phase Locked Loop (PLL)* [4], [5], [15], [17]–[19] or a *Frequency Locked Loop (FLL)* [8], [16], [20], [21] to estimate the signal's frequency online.

Hereby, several SOGIs with different oscillation frequencies can be parallelized to decompose a distorted input signal into its harmonic components. Although the grid norms IEC/EN 61000-3-2 (for currents up to the 40^{th} harmonic) and EN 50160 (for voltages up to the 25^{th} harmonic) require the consideration of a large number of harmonics, this decomposition of distorted grid signals into *multiple* (more than two or three) harmonics is usually not considered. Common approach is to filter out higher order harmonics which induces a delay into the estimation and/or synchronisation process and may even endanger stability/functionality of the closed-loop power control.

Only few papers [7], [12], [14], [15], [22]–[26] explicitly deal with multiple harmonics. In [14], an input signal with six harmonics and varying fundamental frequency was considered; the overall estimation time took about 1.5 s. Additionally, the authors proved the stability of the parallelized SOGI system (without considering the FLL) but did not give a reasonable tuning rule for their observer. [23] used a total of four harmonics and included frequency estimation but also missed to provide guidelines for a good tuning. [24] analyzed up to nine harmonics without considering frequency adaption or tuning parameters; moreover, the implementation of the observer was not thoroughly discussed. In [12], a modification of the parallelized SOGIs was discussed to robustify their performance under frequency fluctuations; however, frequency adaption itself was not considered. Seven harmonics were considered for validation. In [25], a thorough stability analysis of parallelized SOGIs was presented and tuning options were discussed in detail. But, still, the settling time of the estimation algorithm was too long with about 120 ms. Besides frequency adaption and ten harmonics, the presence of a dc-offset was considered in combination with parallelized SOGIs which is, to the best knowledge of the authors, *one of the very few publications* so far which considers dc-offset and multiple harmonics. In [15] and [22], a Kalman estimator based filtering is proposed which also allows to estimate dc-offset and harmonics within >60 ms; however only *odd* harmonics up the *third* and *thirteenth* order were considered, respectively. In this regard, [25] could be seen as the *only* publication so far which treats estimation of frequency, dc-offset and arbitrarily many (odd and even) harmonics.

Most of the mentioned papers above have in common that they use the so called *standard SOGI (sSOGI)* with solely *one* gain which only allows for a limited tuning and yields a rather slow estimation performance ($>40-50$ ms). In [7], this tuning problem of the sSOGI was solved by introducing a so called *modified SOGI (mSOGI)* with *two* gains which allows "(theoretically) for an arbitrarily fast estimation". Nevertheless, a dc-offset was not considered. Note that also in [15] and [22], two feedback gains per harmonic component were intrinsically used in the proposed Kalman estimator design. A different approach was shown in [26], where a new estimation method based on a similarity transformation was introduced with which an overall stability proof was possible. However, the authors only considered three harmonic components and did neglect a dc-offset.

In contrast to harmonics estimation, the consideration of dc-offsets in the input signal is more present in the literature; however, the explicit estimation or rejection of the dc-offset is dealt with in rather few publications [1], [15], [22], [27], [28]. A good overview of parameter estimation methods in presence of dc-offset is given in [28], but dc-offset estimation itself is not its focus. All methods described use a standard SOGI as prefilter. Some selected methods are

i) the cascaded SOGI: the first SOGI rejects the dc-offset in its estimated input which therefore can be fed straightforward to the next SOGI; ii) the DC-SOGI: this method includes, besides the SOGI, a parallel estimation of the dc-offset; and iii) SOGIs with subsequent calculations like Delayed Signal Cancellations and Complex Coefficient Filters. In [27], several methods aiming at explicit dc-offset estimation are presented. They include (i) a three-phase Phase Locked Loop, (ii) a common DC-SOGI (as in [1], [28]) with frequency adaption and (iii) a transformed DC-SOGI for amplitude-phase and frequency estimation. All methods have in common that (a) they are *not* designed for harmonics estimation (no parallelized SOGIs) and (b) they use the slow *standard* SOGIs with limited tuning capability. Exceptions are [15], [22] where a Kalman estimator-based filter approach has been proposed in combination with a PLL. However, the theoretical derivation and the experimental results are limited to dc-offset, fundamental component and odd harmonics (up to the third and thirteenth order only, respectively).

Finally, frequency estimation can be achieved either by *Phase Locked Loops (PLLs)* [15], [22], [27], [29], [30] or *Frequency Locked Loops (FLLs)* [20], [31]–[33]. In the presence of dc-offsets, the classic frequency adaption is not possible anymore, so in [28] (see above), multiple PLL designs are discussed. In contrast to these publications with PLL, in this paper, frequency estimation by a PLL will not be considered any further and the use of an FLL will be discussed.

The frequency adaption is the *bottleneck* of the estimation process since it significantly decelerates the settling time of the overall estimation (e.g. [15]: $250-600$ ms, [14]: 1500 ms; [25]: 120 ms; or [27]: 60 ms). Moreover, the presented *standard FLLs (sFLLs)* can get locked at zero frequency or even become unstable. In general, its performance is highly dependent on amplitudes and frequencies of the signals to be analyzed. To encounter these problems, several approaches have been reported this far. One is called *Gain Normalization (GN)* [34] and normalizes the frequency adaption in view of signal amplitudes. This approach was further extended by Output Saturation [10], [25] and was finally upgraded to an FLL with GN, sign-correct *Anti-Windup (AW)* decision function and *Rate Limitation (RL)* in [7] to prevent overshooting and achieve a more robust and stable performance.

To the best knowledge of the authors, only their own alternative work [25] deals with the estimation of dc-offset, arbitrarily many (odd *and* even) harmonic components *and* frequency adaption. Unfortunately, the proposed approach has a (very) slow settling time and its implementation is rather complicated. That is why this article proposes an overall estimation system – the *Frequency Adaptive Observer (FAO)* — which is capable of estimating (i) dc-offset, (ii) fundamental frequency and (iii) all (known) harmonic components with *fast* estimation performance but with a *simpler* implementation than [25]. Moreover, for known frequencies, the FAO can be tuned such that it can estimate all parameters with a prescribed settling time. Concluding, the contributions of this paper are extensions of [7] and can be summarized as follows:

i) Introduction of a generic and parallelized observer structure consisting of *DC-Integrator (DCI)* and *modified Second-Order Generalized Integrators (mSOGIs)* and the *analytical* computation of the observer gains which achieves a prescribed settling time by pole placement (see Section III-D);
ii) Extensions of the *modified Frequency Locked Loop (mFLL)* with low-pass filters, gain normalization, anti-windup and rate limitation for proper functionality in combination with the parallelized DCI+mSOGIs leading to the overall FAO (see Section III-E);
iii) Implementation and experimental validation of the proposed parallelized DCI+mSOGIs and the overall FAO in comparison to the existing parallelized sSOGI+sFLL system without dc-offset estimation and a non-parallelized DC+sSOGI+sFLL system (see Section IV).

II. PROBLEM STATEMENT

A single-phase grid signal

$$\forall t \geq 0: \quad y(t) := \underbrace{a_0(t)}_{=:y_0(t)} + \sum_{\nu \in \mathbb{H}_\nu} \underbrace{a_\nu(t)\cos(\phi_\nu(t))}_{:=y_\nu(t)} \tag{1}$$

with dc-offset y_0 and arbitrarily many harmonic components y_ν is considered, where $\mathbb{H}_\nu := \{\nu_1, \nu_2, \ldots, \nu_n\} \subset \mathbb{Q}_{>0}$ is the set of all considered harmonic orders (with fundamental order $\nu_1 = 1$). Note that any harmonic order $\nu \in \mathbb{H}_\nu$ may represent any sub, inter, even or odd harmonic of interest (e.g. $\nu \in \{1, \frac{1}{3}, \frac{8}{5}, 2, 4, 3, 7\}$). For an ideal estimation, all harmonic orders $\nu \in \mathbb{H}_\nu$ must be known in advance. Moreover, the harmonic phase angles

$$\forall \nu \in \mathbb{H}_\nu \, \forall t \geq 0: \quad \phi_\nu(t) := \int_0^t \nu\omega(\tau)\,\mathrm{d}\tau + \phi_{\nu,0}(t)$$

depend on the possibly *time-varying*[1] angular frequency $\omega > 0\,\mathrm{rad\,s^{-1}}$; also, the dc-offset $y_0 = a_0$, the amplitudes a_ν and angles $\phi_{\nu,0}$ are allowed to be *time-varying*. Goal is to estimate y as in (1) by its estimate (indicated by "$\widehat{\ }$")

$$\forall t \geq 0: \quad \widehat{y}(t) := \underbrace{\widehat{a}_0(t)}_{=:\widehat{y}_0(t)} + \sum_{\nu \in \mathbb{H}_\nu} \underbrace{\widehat{a}_\nu(t)\cos\big(\widehat{\phi}_\nu(t)\big)}_{:=\widehat{y}_\nu(t)}, \tag{2}$$

which shall be decomposed into the *estimates* of the harmonic components $\widehat{y}_\nu$ and the dc-offset $\widehat{y}_0 = \widehat{a}_0$, respectively. This estimation requires the estimate $\widehat{\omega}$ of the fundamental angular frequency. To achieve this goal, this paper proposes (i) the parallelization of a *DC-integrator (DCI)* and several *modified SOGIs (mSOGIs)* and (ii) the use of a *modified Frequency Locked Loop (mFLL)* with *Gain Normalization* (GN), sign-correct *Anti-Windup* (AW), *Rate Limitation* (RL) and low-pass filters LPFs. Both lead to the overall FAO for a fast and robust estimation of all grid signal parameters in real time.

[1]The common representation $\phi_\nu = \nu\omega$ is an *unnecessary* simplification.

III. PROPOSED SOLUTION: FREQUENCY ADAPTIVE OBSERVER (FAO)

This section presents the theoretical background for the development and implementation of the FAO. It consists of the parallelization of mSOGIs (as introduced in [7]) and a DCI. The development follows a thorough derivation in state space as the widespread use of transfer function or the analysis in the frequency domain should be avoided, as those are limited to linear systems only. However, the proposed FAO is a *nonlinear* observer and it represents a *generalization* of the parallelization,[2] of sSOGIs and sFLL as proposed in [23]. Moreover, an explicit implementation of the harmonic decoupling network (HDN), as proposed in [23], is *not* required.

The principle idea of the FAO is based on the Internal Model Principle (as introduced by Wonham in the 1980s [35]). The internal model principle is usually a key tool to solve tracking and/or disturbance rejection problems in feedback loops. For the considered estimation/observation problem in this paper, the Internal Model Principle can be re-interpreted in the following way: For any given exogenous (input) signal y as in (1), the observation/estimation problem can be solved by equipping a dynamical *generating system* with *feedback*. The generating system must be capable of *reduplicating* the exogenous signal y and, hence, can be considered as an adequately designed internal model.

A. GENERATING SYSTEM (INTERNAL MODEL)

Note that any constant (such as the dc-offset a_0) can be generated by the following integrator

$$\tfrac{\mathrm{d}}{\mathrm{d}t}x_0(t) = 0 \cdot x_0(t), \quad x_0(0) = x_{0,0}, \quad y_0(t) = 1 \cdot x_0(t), \tag{3}$$

with zero input and appropriate initial value $x_{0,0}$. Moreover, any sinusoidal signal y_ν (e.g. the ν-th harmonic component) and its respective quadrature signal q_ν can be reduplicated by the following second-order dynamical system

$$\left.\begin{aligned} \tfrac{\mathrm{d}}{\mathrm{d}t}\overbrace{\begin{pmatrix} x_\nu(t) \\ q_\nu(t) \end{pmatrix}}^{=:\boldsymbol{x}_\nu(t)\in\mathbb{R}^2} &= \omega \overbrace{\begin{bmatrix} 0 & -\nu \\ \nu & 0 \end{bmatrix}}^{=:\boldsymbol{J}_\nu\in\mathbb{R}^{2\times 2}} \boldsymbol{x}_\nu(t), \quad \boldsymbol{x}_\nu(0) = \boldsymbol{x}_{\nu,0}, \\ y_\nu(t) &= \underbrace{\begin{pmatrix} 1, & 0 \end{pmatrix}}_{=:\boldsymbol{c}_\nu^\top\in\mathbb{R}^2} \boldsymbol{x}_\nu(t), \end{aligned}\right\} \tag{4}$$

which represents an harmonic oscillator. Amplitude a_ν and phase angle ϕ_ν are determined by the initial values in $\boldsymbol{x}_{\nu,0}$. The overall generating system, which is able to reduplicate y as in (1), consists of the parallelization of (3) and (4). Hence,

[2]In [23] the parallelized sSOGIs with sFLL were called *multiple* SOGIs with FLL (MSOGI-FLL); which must not be confused with mSOGIs.

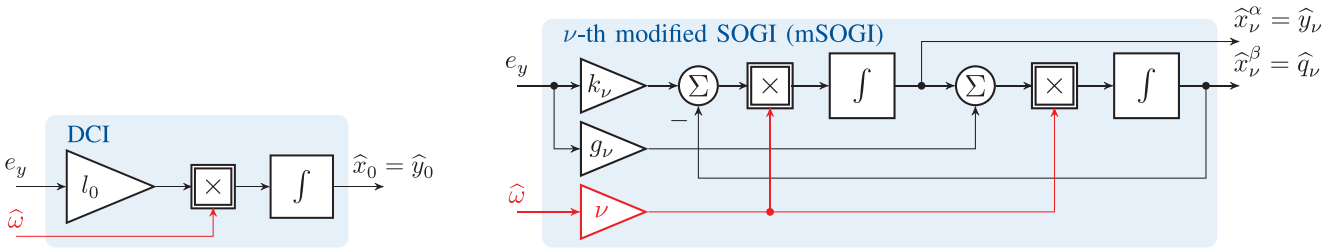

(a) Block diagram of DC-integrator (DCI). (b) Block diagram of ν-th modified Second-order Generalized Integrator (mSOGI) [7].

FIGURE 1. Components of the Frequency Adaptive Observer (FAO): (a) DC-Integrator (DCI) and (b) modified SOGI (mSOGI).

its dynamics are given by (cf. [7]; there without x_0)

$$\left.\begin{aligned} \frac{\mathrm{d}}{\mathrm{d}t}\overbrace{\begin{pmatrix} x_0(t) \\ \boldsymbol{x}_1(t) \\ \boldsymbol{x}_{\nu_2}(t) \\ \vdots \\ \boldsymbol{x}_{\nu_n}(t) \end{pmatrix}}^{=:\boldsymbol{x}(t)\in\mathbb{R}^{2n+1}} &= \omega \overbrace{\begin{bmatrix} 0 & \boldsymbol{0}_2^\top & \boldsymbol{0}_2^\top & \cdots & \boldsymbol{0}_2^\top \\ \boldsymbol{0}_2 & \boldsymbol{J}_{\nu_1} & \boldsymbol{O}_{2\times 2} & \cdots & \boldsymbol{O}_{2\times 2} \\ \boldsymbol{0}_2 & \boldsymbol{O}_{2\times 2} & \boldsymbol{J}_{\nu_2} & \cdots & \boldsymbol{O}_{2\times 2} \\ \vdots & \vdots & \vdots & \ddots & \vdots \\ \boldsymbol{0}_2 & \boldsymbol{O}_{2\times 2} & \boldsymbol{O}_{2\times 2} & \cdots & \boldsymbol{J}_{\nu_n} \end{bmatrix}}^{=:\boldsymbol{J}\in\mathbb{R}^{(2n+1)\times(2n+1)}} \boldsymbol{x}(t) \\ y(t) &= \underbrace{\left(1,\, \boldsymbol{c}_{\nu}^\top,\, \ldots,\, \boldsymbol{c}_{\nu}^\top\right)}_{=:\boldsymbol{c}^\top\in\mathbb{R}^{2n+1}} \boldsymbol{x}(t). \end{aligned}\right\} \tag{5}$$

If all initial values in $\boldsymbol{x}(0) = \boldsymbol{x}_0$ and the angular frequency ω were known, then (5) could perfectly reduplicate the single-phase signal y as in (1). But, since those values are *not* known a priori, an observer must be designed which is actually feasible since the dynamics (5) are fully state observable, i.e.

$$\operatorname{rank}\left[\boldsymbol{c}, \quad \boldsymbol{J}^\top\boldsymbol{c}, \quad \cdots, \quad (\boldsymbol{J}^\top)^{2n}\boldsymbol{c}\right]^\top = 2n+1;$$

as a straight forward extension of the proof in [36] shows.

B. DC-INTEGRATOR (DCI)

To estimate the dc-offset online, the generating system (3) is equipped with feedback

$$-\widehat{\omega}(t) l_0 e_y(t) = -\widehat{\omega}(t) l_0 \left(y(t) - \widehat{y}(t)\right)$$

of the estimation error $e_y := y - \widehat{y}$ (difference between input signal y and its estimate $\widehat{y}$ of the FAO, see Section III-D), leading to the DC-Integrator (DCI) dynamics

$$\left.\begin{aligned} \tfrac{\mathrm{d}}{\mathrm{d}t}\widehat{x}_0(t) &= \widehat{\omega}(t)\, l_0 \underbrace{\left(y(t) - \widehat{y}(t)\right)}_{=e_y(t)}, \quad \widehat{x}_0(0) = 0 \\ \widehat{y}_0(t) &= \widehat{x}_0(t) \end{aligned}\right\} \tag{6}$$

which is a simple first-order system (see Fig. 1(a)) which, if y is constant, achieves $\widehat{y} \to y$ and can be arbitrarily tuned by the gain $l_0 > 0$. The estimated angular frequency $\widehat{\omega}(t)$ scales the system dynamics and is obtained by the *modified Frequency Locked Loop (mFLL)* (see Section III-E). For non-constant (sinusoidal) components in y, the DCI acts as an (adaptive) low-pass filter to estimate the DC-offset y_0; whereas its combination with the parallelized mSOGIs allows to estimate dc-offset and harmonics at the same time (as will be discussed in Section III-D).

C. MODIFIED SECOND-ORDER GENERALIZED INTEGRATOR (MSOGI)

The *modified Second-Order Generalized Integrator (mSOGI)* was proposed in [7]. It is a *generalization* of the commonly used *standard SOGI (sSOGI)* as e.g. implemented in [16] for multiple harmonics estimation. The mSOGI achieves an arbitrarily fast estimation performance since *two* gains are available for tuning; in contrast to the sSOGI which can be tuned solely by *one* gain [16], [34].

To obtain the mSOGI dynamics and to estimate the ν-th sinusoidal-like harmonic component $\widehat{y}_\nu$, the internal model in (4) is used with the estimated $\widehat{\omega}$ instead of ω and is equipped with the feedback

$$-\widehat{\omega}(t)\underbrace{\begin{pmatrix} \nu\, k_\nu \\ \nu\, g_\nu \end{pmatrix}}_{=:\boldsymbol{l}_\nu} \underbrace{\left(y(t) - \widehat{y}(t)\right)}_{=e_y(t)}$$

of the estimation error e_y (as the DCI), which yields the mSOGI dynamics (for details see [7] and Fig. 1(b))

$$\left.\begin{aligned} \frac{\mathrm{d}}{\mathrm{d}t}\overbrace{\begin{pmatrix} \widehat{x}_\nu^\alpha(t) \\ \widehat{x}_\nu^\beta(t) \end{pmatrix}}^{=:\widehat{\boldsymbol{x}}_\nu(t)} &= \widehat{\omega}(t)\boldsymbol{J}_\nu\widehat{\boldsymbol{x}}_\nu(t) + \widehat{\omega}(t)\boldsymbol{l}_\nu \overbrace{\left(y(t) - \widehat{y}(t)\right)}^{=e_y(t)} \\ \widehat{y}_\nu(t) &= \boldsymbol{c}_\nu^\top\widehat{\boldsymbol{x}}_\nu(t). \end{aligned}\right\} \tag{7}$$

The state vector $\widehat{\boldsymbol{x}}_\nu$ of the ν-th mSOGI consists of estimated in-phase signal $\widehat{x}_\nu^\alpha = \widehat{y}_\nu$ and estimated quadrature signal $\widehat{x}_\nu^\beta = \widehat{q}_\nu$ of the ν-th harmonic component. The purpose of the mSOGI – similar to the sSOGI – is to estimate a given sinusoidal signal y_ν and its quadrature signal q_ν such that $\widehat{y}_\nu \to y_\nu$ and $\widehat{q}_\nu \to q_\nu$ (if $y = y_\nu$). Its working principle is based on the oscillating nature of its dynamics whose resonance frequency is the harmonic angular frequency $\nu\widehat{\omega}$.

Note that the mSOGI compared to the sSOGI achieves a (much) faster estimation, since its poles can be chosen arbitrarily as the *two* feedback gains k_ν and g_ν are available for tuning instead of only *one* feedback gain k_ν for the sSOGI (with $g_\nu = 0$ [7], [34]).

Since, in most cases, the input signal y compromises dc-offset and multiple harmonics, the parallelization of DCI and multiple mSOGIs is necessary as will be discussed next.

D. PARALLELIZATION OF DCI AND MSOGIS

As already noted, only the overall signal y as in (1), the sum of dc-offset y_0 and harmonics y_ν, is measured and fed to the overall observer. Hence, to achieve a proper estimation of all components, a parallelized structure must be set up (see Fig. 4).

To do so, for dc-offset and all harmonic orders $\nu \in \mathbb{H}_\nu$, DCI (6) and mSOGIs (7) are merged and parallelized leading to the overall observer dynamics

$$\left.\begin{aligned} \tfrac{\mathrm{d}}{\mathrm{d}t}\widehat{\boldsymbol{x}}(t) &= \widehat{\omega}(t)\left[\boldsymbol{J}-\boldsymbol{l}\boldsymbol{c}^\top\right]\widehat{\boldsymbol{x}}(t)+\widehat{\omega}(t)\boldsymbol{l}y(t), \quad \widehat{\boldsymbol{x}}(0)=\widehat{\boldsymbol{x}}_0,\\ \widehat{y}(t) &= \boldsymbol{c}^\top\widehat{\boldsymbol{x}}(t) \end{aligned}\right\} \tag{8}$$

where $\widehat{\boldsymbol{x}} := (\widehat{x}_0, \widehat{\boldsymbol{x}}_{\nu_1}^\top, \ldots, \widehat{\boldsymbol{x}}_{\nu_n}^\top)^\top \in \mathbb{R}^{2n+1}$ and $\boldsymbol{l} := (l_0, \boldsymbol{l}_{\nu_1}^\top, \ldots, \boldsymbol{l}_{\nu_n}^\top)^\top \in \mathbb{R}^{2n+1}$ consist of all sub-states and sub-feedback gains of DCI and mSOGIs, respectively. Clearly, in (8), only the available and measured signal y is used for feedback. Note that this generic observer structure for dc-offset and arbitrary harmonics estimation using DCI+mSOGIs has *not* yet been proposed and derived for the general case (arbitrary order) in literature and validated by extensive measurement results (as will be done in Section IV). In [1], [28], the trivial observer structure for dc-offset and fundamental signal estimation (i.e. $n = 1$) has been discussed. In [15] and [22], a similar approach (called Kalman estimator-based filter) was proposed but only derived and validated for a signal consisting of fundamental, odd harmonics (up to the third and thirteenth order, respectively) and dc-offset.

Moreover, the tedious-to-implement harmonic decoupling network (HDN) as proposed in [23] is *not* required; as the estimation error $e_y = y - \widehat{y}$ is directly fed to the DCI and *all* mSOGIs (see Fig. 4). The implementation is rather simple, since the parallelization of DCI and mSOGIs can be implemented in a compact way using the state space representation in (8). There is no need to implement and interconnect DCI and each mSOGI individually or separately.

Furthermore, in contrast to parallelized sSOGIs with only one gain per sSOGI, the tuning of the parallelized DCI and mSOGIs in (8) is very simple and gives the necessary $2n+1$ degrees of freedom as $2n+1$ tuning parameters are available. In contrast to that, for a parallelized *sSOGI* design (with $g_\nu = 0$ for all $\nu \in \mathbb{H}_\nu$), the feedback vector $\boldsymbol{l} = (l_0, \nu_1 k_{\nu_1}, 0, \ldots, \nu_n k_{\nu_n}, 0)^\top$ has only $n+1$ gains whereas the obverser matrix $\boldsymbol{J} - \boldsymbol{l}\boldsymbol{c}^\top$ still has $2n+1$ eigenvalues (poles). Hence, *solely* the observer with parallelized mSOGIs allows for an arbitrary tuning by pole placement (or linear quadratic regulator (LQR) design [15]). Pole placement can be easily achieved by MATLAB which provides the `place` command, i.e.

$$\boldsymbol{l}^\top = \texttt{place}\big(\boldsymbol{J}^\top,\ \boldsymbol{c},\ \boldsymbol{p}^\star\big), \tag{9}$$

which allows to assign the (desired) eigenvalues $\boldsymbol{p}^\star := (p_0^\star, p_{\nu_1}^\star, \overline{p}_{\nu_1}^\star, \ldots, p_{\nu_n}^\star, \overline{p}_{\nu_n}^\star)^\top \in \mathbb{R}^{2n+1}$ of the observer matrix $\boldsymbol{J} - \boldsymbol{l}\boldsymbol{c}^\top$. The vector $\boldsymbol{p}^\star$ contains the desired poles $p_0^* \in \mathbb{R}$ of the DCI and the desired poles $p_\nu^\star, \overline{p}_\nu^\star \in \mathbb{C}$ of the parallelized mSOGIs for all $\nu \in \{\nu_1, \ldots, \nu_n\}$. However, this command requires that the multiplicity of the poles is *not* greater than $\operatorname{rank}(\boldsymbol{c}) = 1$. If, for some reason, this is desired, one could take advantage of the following (proposed) *analytic* gain calculation

$$\boldsymbol{l} = \begin{bmatrix} \boldsymbol{0}_{2n}^\top & \frac{1}{\prod_{\nu\in\mathbb{H}_n}\nu^2} \\ \boldsymbol{S} & -\frac{1}{\prod_{\nu\in\mathbb{H}_n}\nu^2}\boldsymbol{S}\boldsymbol{w} \end{bmatrix} \widetilde{\boldsymbol{p}}_{\boldsymbol{A}}^\star \tag{10}$$

with $\boldsymbol{R}_i := \begin{bmatrix} 1 & 0 \\ 0 & -\frac{1}{\nu_i} \end{bmatrix}$, $\boldsymbol{S} := \begin{bmatrix} \boldsymbol{S}_{1,1} & \cdots & \boldsymbol{S}_{n,1} \\ \vdots & \ddots & \vdots \\ \boldsymbol{S}_{1,n} & \cdots & \boldsymbol{S}_{n,n} \end{bmatrix}$, $\boldsymbol{S}_{c,r} := (-1)^{c+1}\nu_r^{2(n-c)}\boldsymbol{R}_r \prod_{\substack{i=1\\ i\neq r}}(\nu_r^2 - \nu_i^2)^{-1}$, $\boldsymbol{w} := (1,\ 0,\ \sum_{\nu\in\mathbb{H}_n}\nu^2,\ 0,\ \ldots,\ \sum_{\nu\in\mathbb{H}_n}\prod_{\substack{\mu\in\mathbb{H}_n\\ \mu\neq\nu}}\mu^2,\ 0)^\top$ and $\widetilde{\boldsymbol{p}}_{\boldsymbol{A}}^\star := (-\sum_{i=1}^{2n+1} p_i^\star,\ \sum_{i=1}^{2n+1} p_i^\star \sum_{j=i+1}^{2n+1} p_j^\star - \sum_{\nu\in\mathbb{H}_n}\nu^2,\ \ldots,\ \sum_{i=1}^{2n+1}\prod_{\substack{j=1\\ j\neq i}}^{2n+1} p_j^\star - \prod_{\nu\in\mathbb{H}_n}\nu^2,\ -\prod_{i=1}^{2n+1} p_i^\star)^\top$ which is an extension of Eq. (15) in [36].

A good tuning is achieved by the choices $p_0^\star \leq \min_\nu \Re(p_\nu^\star)$, $p_\nu^\star = -\sigma^\star + \jmath\nu^\star$ and $\overline{p}_\nu^\star = -\sigma^\star - \jmath\nu^\star$ with $\sigma^\star > 0$ (e.g. $\sigma^\star = \frac{3}{2}$ or 2) and $\nu^\star = \nu \in \mathbb{H}_\nu$ to preserve a (damped) oscillating behavior of the mSOGIs. Since the eigenvalue(s) or pole(s) closest to the imaginary axis (i.e. those poles with $\max_\nu \Re(p_i^\star)$) determine the overall settling time of the parallelized DCI+mSOGIs system, the minimum settling time can (theoretically) be set arbitrarily. However, noise sensitivity and overshooting may limit the achievable response; in particular since the overall poles of the varying matrix $\widehat{\omega}(t)[\boldsymbol{J} - \boldsymbol{l}\boldsymbol{c}^\top]$ are scaled by the estimate $\widehat{\omega}(t)$.

E. FREQUENCY ADAPTION BY MODIFIED FLL (MFLL)

The last ingredient of the FAO is the estimation or – more precisely – the adaption of the angular frequency by the *modified Frequency Locked Loop (mFLL)*. Goal is to achieve asymptotic adaption of $\widehat{\omega}(t)$ such that $\widehat{\omega} \to \omega$. The principle adaption law

$$\tfrac{\mathrm{d}}{\mathrm{d}t}\widehat{\omega}(t) \propto \gamma(t)\underbrace{\big(y(t)-\widehat{y}(t)\big)}_{=:e_y(t)}\boldsymbol{\lambda}^\top\widehat{\boldsymbol{x}}(t), \qquad \widehat{\omega}(0)=\widehat{\omega}_0 \tag{11}$$

of the mFLL is based on a steady-state analysis of the parallelized DCI and mSOGIs (similar to the analysis in [36]). The selection vector $\boldsymbol{\lambda} := (0,\ g_{\nu_1},\ -k_{\nu_1},\ 0,\ \ldots,\ 0)^\top \in \mathbb{R}^{2n+1}$ extracts only the fundamental components of the estimated in-phase signal $\widehat{y}_{\nu_1}$ and its quadrature signal $\widehat{q}_{\nu_1}$ such that the product $e_y\boldsymbol{\lambda}^\top\widehat{\boldsymbol{x}} = e_y\boldsymbol{l}_{\nu_1}^\top\boldsymbol{J}_{\nu_1}\widehat{\boldsymbol{x}}_{\nu_1}$ is *in-phase* with the input estimation error $e_y = y - \widehat{y}$. Observe the inverse weighting of $\widehat{y}_{\nu_1}$ by g_{ν_1} and $\widehat{q}_{\nu_1}$ by $-k_{\nu_1}$. The adaption in (11) achieves (on average over one fundamental period) a sign-correct adaption

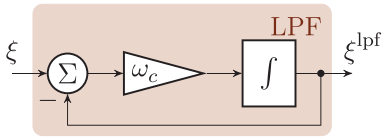

FIGURE 2. Block diagram of the low-pass filters (LPFs) used in the mFLL.

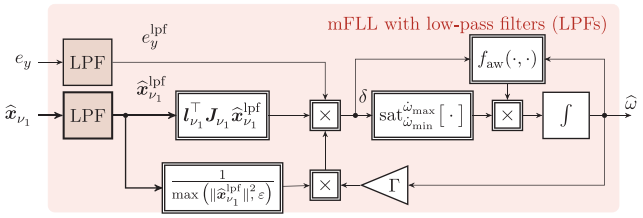

FIGURE 3. Block diagram of modified Frequency Locked Loop (mFLL) with gain normalization (GN), sign-correct anti-windup (AW) decision function, rate limitation (RL) and low-pass filters (LPFs).

of the angular frequency estimate $\widehat{\omega}$ for all positive gains $\gamma(t) > 0$. The initial value $\widehat{\omega}_0$ helps to improve the transient behavior of the mFLL; e.g. in Europe, the nominal frequency is $f_0 = 50\,\mathrm{Hz}$, therefore the initial (nominal) value should be $\omega_0 = 2\pi\, f_0$.

As proposed in [7], the principle adaption law (11) should be extended by (i) a gain normalization (GN), (ii) a sign-correct anti-windup (AW) decision function

$$f_{\mathrm{aw}}(\widehat{\omega}, \delta) := \begin{cases} 0, & \text{for } \left(\widehat{\omega} \geq \omega_{\max} \wedge \delta \propto \frac{\mathrm{d}}{\mathrm{d}t}\widehat{\omega} \geq 0\right) \\ & \quad \vee \left(\widehat{\omega} \leq \omega_{\min} \wedge \delta \propto \frac{\mathrm{d}}{\mathrm{d}t}\widehat{\omega} \leq 0\right) \\ 1, & \text{else} \end{cases} \tag{12}$$

and (iii) a rate limitation (RL)

$$\mathrm{sat}_{\dot{\omega}_{\min}}^{\dot{\omega}_{\max}}[\delta] := \begin{cases} \dot{\omega}_{\max}, & \delta > \dot{\omega}_{\max} \\ \delta, & \dot{\omega}_{\min} \leq \delta \leq \dot{\omega}_{\max} \\ \dot{\omega}_{\min}, & \delta < \dot{\omega}_{\min} \end{cases} \tag{13}$$

to achieve a stable and smooth(er) frequency estimation. In these functions, the upper and lower limits $\omega_{\max}$, $\omega_{\min}$, $\dot{\omega}_{\max}$ and $\dot{\omega}_{\min}$ guarantee that the frequency estimate $\widehat{\omega}$ is (i) always bounded away from zero (crucial for stability of the FAO) and stays within the interval $[\omega_{\min}, \omega_{\max}]$ and (ii) the adaption is not *too* fast yielding a more robust adaption (for details see [7]). Moreover, in view of measurement noise, additional low-pass filters (LPFs) should be included in the mFLL. The considered LPFs (see Fig. 2) have cut-off frequency ω_c and the following first-order dynamics

$$\frac{\mathrm{d}}{\mathrm{d}t}\xi^{\mathrm{lpf}}(t) = -\omega_c \xi^{\mathrm{lpf}}(t) + \omega_c \xi(t), \qquad \xi^{\mathrm{lpf}}(0) = 0. \tag{14}$$

Three LPFs should be implemented for the three signals e_y, $\widehat{y}_{\nu_1}$ and $\widehat{q}_{\nu_1}$ to achieve synchronicity (identical phase lag) of all filtered signals e_y^{lpf}, $\widehat{y}_{\nu_1}^{\mathrm{lpf}}$ and $\widehat{q}_{\nu_1}^{\mathrm{lpf}}$, respectively. Bringing all together, finally, leads to the mFLL as illustrated in Fig. 3 with

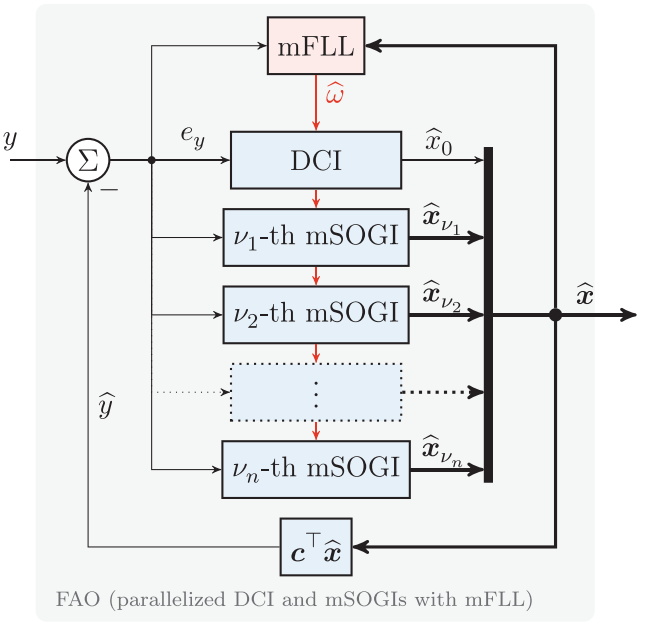

FIGURE 4. Block diagram of the Frequency Adaptive Observer (FAO).

the overall adaption law

$$\frac{\mathrm{d}}{\mathrm{d}t}\widehat{\omega}(t) = f_{\mathrm{aw}}\big(\widehat{\omega}(t), \delta(t)\big)\ \mathrm{sat}_{\dot{\omega}_{\min}}^{\dot{\omega}_{\max}}\overbrace{\left[\frac{\Gamma\, \widehat{\omega}(t)\, e_y^{\mathrm{lpf}}(t)\, \boldsymbol{l}_{\nu_1}^\top \boldsymbol{J}_\nu \widehat{\boldsymbol{x}}_{\nu_1}^{\mathrm{lpf}}(t)}{\max\left(\left\|\widehat{\boldsymbol{x}}_{\nu_1}^{\mathrm{lpf}}(t)\right\|^2, \varepsilon\right)}\right]}^{=:\delta(t)} \tag{15}$$

with some *constant* gain $\Gamma > 0$.

Concluding, note that the *standard FLL (sFLL)* [34], which is usually implemented, comes only with GN but *without* AW, RL and LPFs; which has several drawbacks as discussed in [7].

F. OVERALL STRUCTURE OF FAO

The block diagram of the complete FAO, consisting of parallelized DCI (6) and mSOGIs (7), and mFLL (15) is illustrated in Fig. 4. The FAO is fed by the input y as in (1) and provides the estimates $\widehat{y}$ as in (2) and $\widehat{\omega}$ (according to adaption as in (15)), and the overall estimation state vector $\widehat{\boldsymbol{x}} = (\widehat{x}_0, \widehat{y}_{\nu_1}, \widehat{q}_{\nu_1}, \ldots, \widehat{y}_{\nu_n}, \widehat{q}_{\nu_n})^\top$, which contains the (i) dc-offset estimate $\widehat{y}_0 = \widehat{x}_0 = \widehat{a}_0$ and, for $\nu \in \mathbb{H}_\nu$, (ii) all harmonic in-phase $\widehat{y}_\nu$ and quadrature $\widehat{q}_\nu$ estimates. Based on the estimated individual harmonic sub-state vector $\widehat{\boldsymbol{x}}_\nu = (\widehat{y}_\nu, \widehat{q}_\nu)^\top$, amplitude estimate $\widehat{a}_\nu := \|\widehat{\boldsymbol{x}}_\nu\|$ and phase angle estimate $\widehat{\phi}_\nu := \arctan 2(\widehat{y}_\nu, \widehat{q}_\nu)$ of each harmonic component can be computed for all $\nu \in \mathbb{H}_\nu$. Note that the mFLL provides the estimated angular frequency $\widehat{\omega}$ to DCI *and* all mSOGIs.

IV. IMPLEMENTATION AND MEASUREMENT RESULTS

To verify the proposed FAO, experimental results are carried out where *three* estimation methods and their estimation performance are compared to each other. The proposed FAO consisting of *DCI, n parallelized mSOGIs and mFLL* (in the

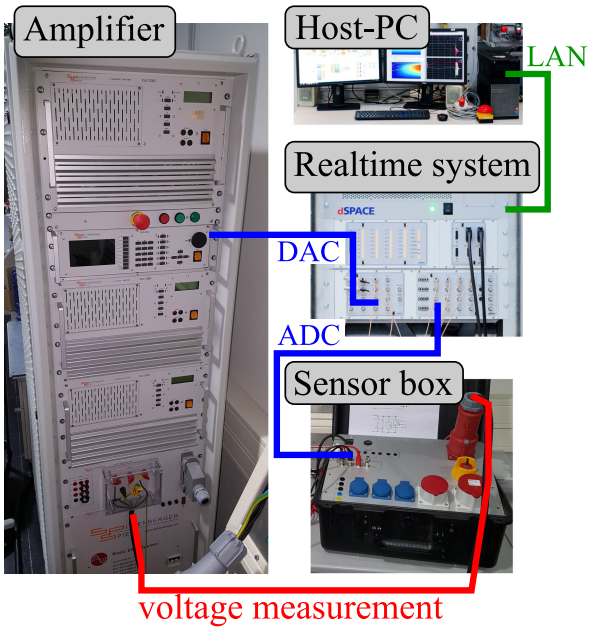

FIGURE 5. Laboratory setup used for comparisons.

following labeled as $\mathbf{mFAO}_{0,n}$) is compared to the only two standard approaches for dc-offset and multiple (odd and even) harmonics estimation available in literature proposed by other researchers this far.[3] The two methods are (i) a simple FAO as proposed in [1] (labeled as $\mathbf{sFAO}_{0,1}$) consisting of a dc-offset estimator (similar to DCI), *one sSOGI* (for fundamental signal only) and *sFLL*, and (ii) a parallelization of n sSOGIs with sFLL but *without* DCI as proposed in [23] (labeled as $\mathbf{sFAO}_{\emptyset,n}$).

The principle structure of the used laboratory setup for the comparisons is illustrated in Fig. 5. For the experiments, the signal to be investigated is generated in Matlab/Simulink R2018b by the internal model (5), which is downloaded via LAN to the dSPACE Processor Board DS1007 where the signal is reproduced in real time, converted from digital to analogue (DAC) by the dSPACE I/O card DS2103, amplified by a Spitzenberger-Spies PAS 5000 four quadrant amplifier, measured by a LEM CV 3–1000 voltage sensor (sensor box) and converted from analogue to digital (ADC) by the dSPACE I/O card DS2004 and, finally, processed by all three estimation methods described above in real time. After the experiment, the measured input signal and estimated quantities are recorded and then analyzed on a Host-PC. The dSPACE system and the amplifier are connected via a ten meters long BNC cable.

Four scenarios for the comparisons will be discussed:

S1): For the first scenario, *one (fundamental) sinusoidal signal with dc-offset and known frequency* is considered. Since frequency is known, all three estimation methods are implemented without FLL. The considered signal undergoes a dc-offset jump of $+100$V at $t = 0.12$ s, an amplitude sag of -75% at $t = 0.24$ s, a phase jump of $-\frac{\pi}{2}$rad at $t = 0.36$ s and reverse jumps in all changed parameters at $t = 0.48$ s (see Figs. 6 and 7).

S2): For the second scenario, an input signal consisting of *dc-offset, fundamental and nine harmonics* with *known frequency* is chosen and fed to all three estimation methods. Since frequency is known, the FLLs are not required and de-activated. The step-like signal parameter changes are identical to Scenario (S1). The results are shown in Figs. 8 and 9.

S3): The third scenario again considers only *one (fundamental) sinusoidal signal with dc-offset* but *with unknown and varying frequency*. Hence, all estimation methods require a FLL to estimate the frequency. The considered signal undergoes frequency jumps of $+2\pi 10\text{rad}\,\text{s}^{-1}$ at $t = 0.12$ s and is shifted about $+\frac{\pi}{2}$rad at $t = 0.24$ s; at $t = 0.36$ s, an error is emulated where the fundamental signal is nullified and only the dc-offset remains. Finally, at $t = 0.48$ s, all signal parameter changes are reversed (see Figs. 10 and 11).

[3]The alternative approach proposed by the authors in [25] is *not* considered for this comparison, since it has a (very) slow estimation performance and is rather complicated to implement and, hence, not being suitable for industrial application.

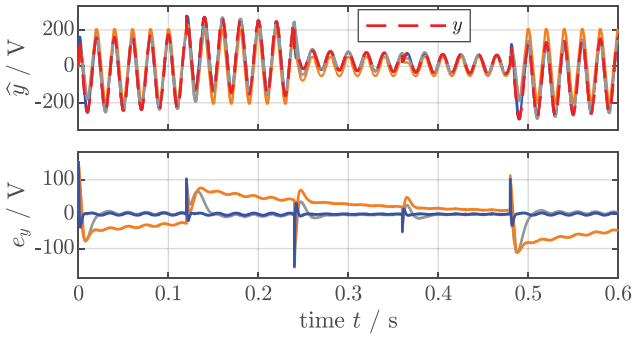

FIGURE 6. Measurement results for Scenario (S1) (fundamental signal with dc-offset and known frequency): The signals shown are input y (- - -), estimate $\hat{y}$ and estimation error $e_y = y - \hat{y}$ of $\mathbf{sFAO}_{0,1}$ (——), $\mathbf{sFAO}_{\emptyset,n}$ (——) and $\mathbf{mFAO}_{0,n}$ (——), respectively.

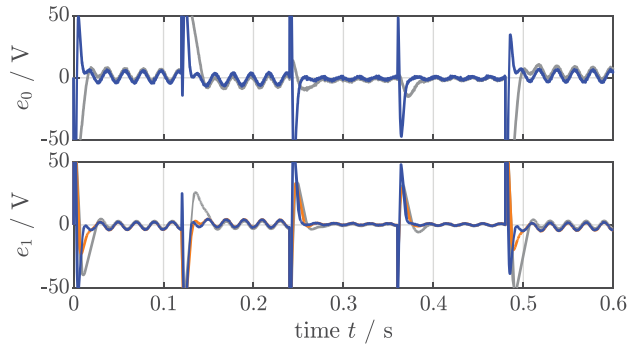

FIGURE 7. Zoomed-in estimation errors of dc-offset and harmonic signal for Scenario (S1) (fundamental signal with dc-offset and known frequency): The signals shown are estimation errors $e_0 = y_0 - \hat{y}_0$ and $e_1 = y_1 - \hat{y}_1$ of $\mathbf{sFAO}_{0,1}$ (——), $\mathbf{sFAO}_{\emptyset,n}$ (——) and $\mathbf{mFAO}_{0,n}$ (——), respectively.

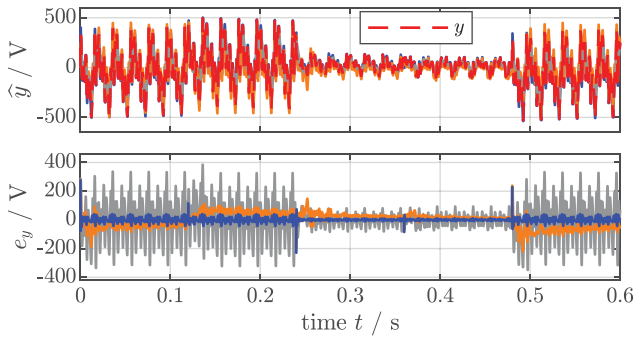

FIGURE 8. **Measurement results for Scenario (S2) (signal with dc-offset, ten harmonics and known frequency): The signals shown are input y (- - -), estimate $\hat{y}$ and estimation error $e_y = y - \hat{y}$ of sFAO$_{0,1}$ (——), sFAO$_{\emptyset,n}$ (——) and mFAO$_{0,n}$ (——), respectively.**

TABLE 1. **Initial Signal Parameters (at $t = 0$) for Scenarios (S2) and (S4)**

ν	0	1	2	3	4	5	6	7	8	9	10
a_ν / V	−50	200	80	40	120	0	80	0	120	40	40
ϕ_ν / rad		0	$\frac{\pi}{2}$	$\frac{3\pi}{2}$	0	$\frac{2\pi}{3}$	$\frac{\pi}{4}$	0	$\frac{5\pi}{4}$	$\frac{5\pi}{3}$	0
ω / $\frac{\text{rad}}{\text{s}}$						$2\pi 50$					

S4): The last scenario uses the signal from Scenario (S2) containing *dc-offset, fundamental and nine harmonics*, but this time, *with unknown and varying frequency* including frequency jumps of $+2\pi 10\text{rad}\,\text{s}^{-1}$ at $t = 0.12\,\text{s}$ and $-2\pi 10\text{rad}\,\text{s}^{-1}$ at $t = 0.48\,\text{s}$. Hence, all estimation methods require a FLL to work properly. The other signal parameter changes are identical to those in Scenario (S3) but, now, all harmonic components are nullified such that only the dc-offset remains for a certain time interval. The estimation results are illustrated in Figs. 12 and 13.

For Scenarios (S1) and (S3), the initial signal parameters (at $t = 0$) are as follows: $a_0 = -50\text{V}$, $a_1 = 200\text{V}$, $\phi_1 = 0\text{rad}$ and $\omega = 2\pi 50\text{rad}\,\text{s}^{-1}$. For Scenarios (S2) and (S4), the respective signal parameters are collected in Table 1. Considering the system parameters, the gains of **sFAO**$_{0,1}$ are taken from [1] and the ones of **sFAO**$_{\emptyset,n}$ are copied from [23]. For the proposed **mFAO**$_{0,n}$, *pole placement* as in (10) is used for tuning such that all poles and eigenvalues of $\boldsymbol{J}$ are shifted by -2 into the negative half plane which is a reasonable compromise between noise sensitivity, overshooting and estimation speed. All system parameters are listed in Table 2.

A. DISCUSSION OF SCENARIO (S1)

For Scenario (S1), a signal with dc-offset, fundamental component (only) and known frequency with step-like changes in the signal parameters is fed to the three FAOs without using the FLLs (which is still implemented but adaption is *turned off*; its initial value is set to the known angular frequency, i.e. $\widehat{\omega} = \omega \Rightarrow \widehat{f} = f$). All three estimation methods,

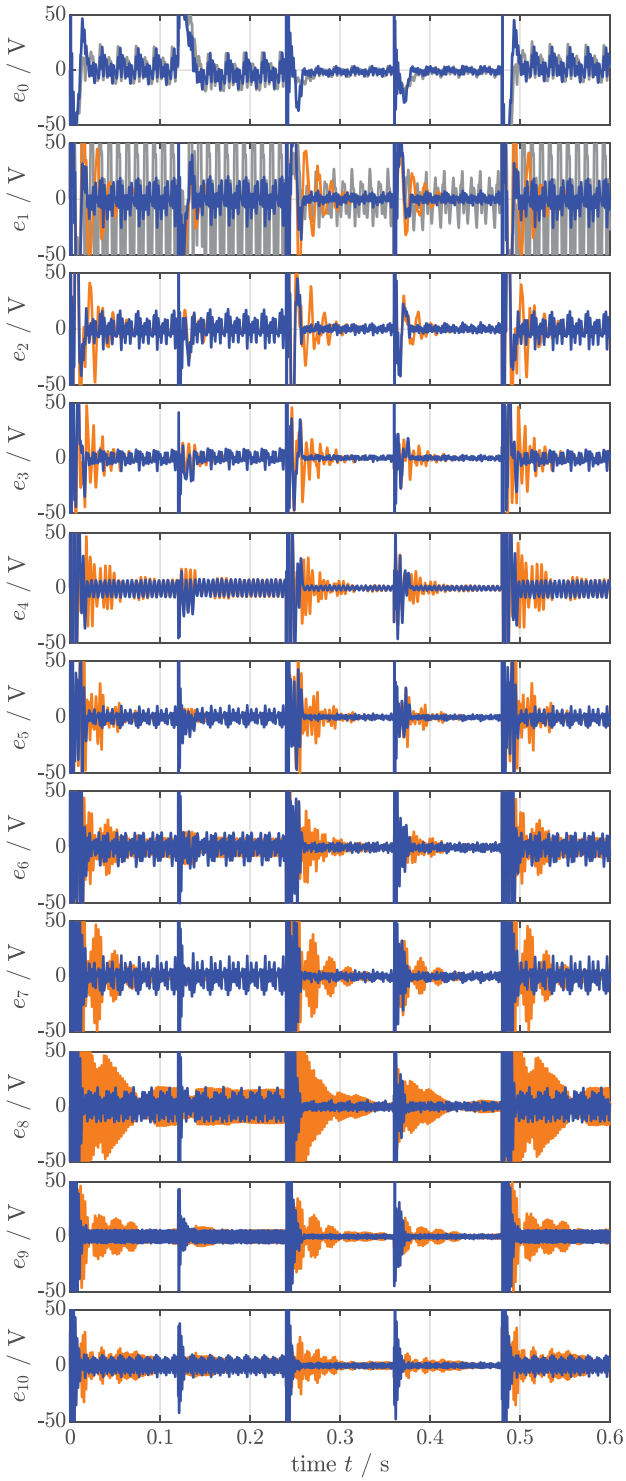

FIGURE 9. **Zoomed-in estimation errors of dc-offset and harmonic signals for Scenario (S2) (signal with dc-offset, harmonics and known frequency): The signals shown are estimation error $e_0 = y_0 - \hat{y}_0$ and $e_\nu = y_\nu - \hat{y}_\nu$ for all $\nu \in \{1, \ldots, 10\}$ of sFAO$_{0,1}$ (——), sFAO$_{\emptyset,n}$ (——) and mFAO$_{0,n}$ (——), respectively.**

i.e. **mFAO**$_{0,n}$, **sFAO**$_{0,1}$ and **sFAO**$_{\emptyset,n}$, are implemented with only *one* SOGI (i.e. $n = 1$).

In Fig. 6, the measurement results for Scenario (S1) are shown. The first subplot shows input y (- - -) and estimated

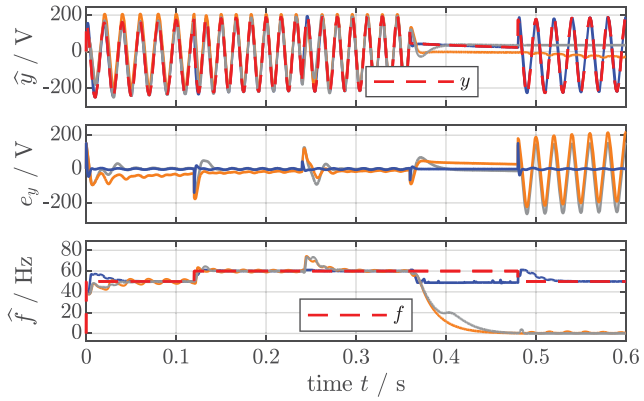

FIGURE 10. Measurement results for Scenario (S3) (fundamental signal with dc-offset and unknown frequency): The signals shown are input y (- - -), estimate $\hat{y}$, estimation error $e_y = y - \hat{y}$, frequency f and its estimate $\hat{f}$ of $\mathbf{sFAO}_{0,1}$ (——), $\mathbf{sFAO}_{\emptyset,n}$ (——) and $\mathbf{mFAO}_{0,n}$ (——), respectively.

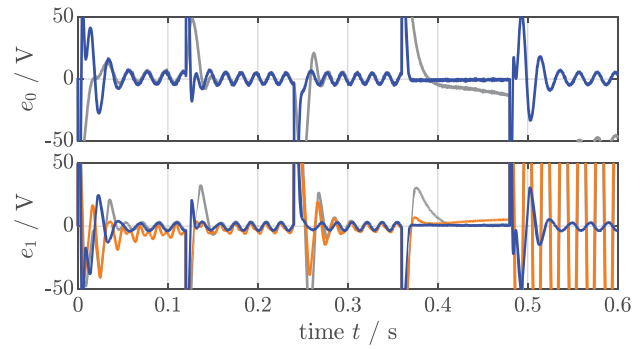

FIGURE 11. Zoomed-in estimation errors of dc-offset and harmonic signal for Scenario (S3) (fundamental signal with dc-offset and *un*known frequency): The signals shown are estimation errors $e_0 = y_0 - \hat{y}_0$ and $e_1 = y_1 - \hat{y}_1$ of $\mathbf{sFAO}_{0,1}$ (——), $\mathbf{sFAO}_{\emptyset,n}$ (——) and $\mathbf{mFAO}_{0,n}$ (——), respectively.

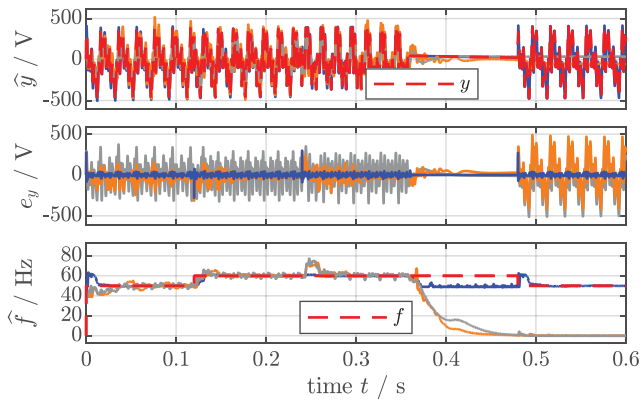

FIGURE 12. Measurement results for Scenario (S4) (signal with dc-offset, ten harmonics and *un*known frequency): The signals shown are input y (- - -) and the estimates $\hat{y}$, the respective estimation errors $e_y = y - \hat{y}$, frequency f and the respective estimates $\hat{f}$ of $\mathbf{sFAO}_{0,1}$ (——), $\mathbf{sFAO}_{\emptyset,n}$ (——) and $\mathbf{mFAO}_{0,n}$ (——).

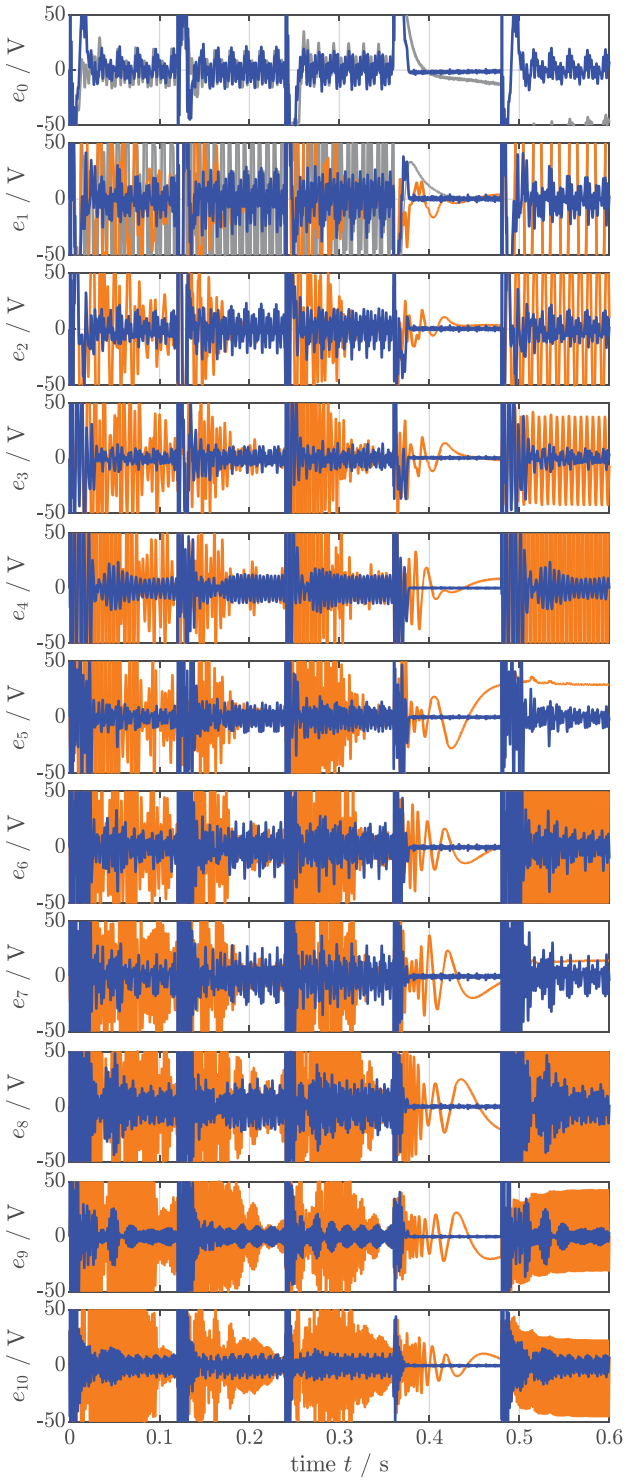

FIGURE 13. Zoomed-in estimation errors of dc-offset and harmonic signals for Scenario (S4) (signal with dc-offset, harmonics and *un*known frequency): The signals shown are the respective estimation errors $e_0 = y_0 - \hat{y}_0$ and $e_\nu = y_\nu - \hat{y}_\nu$ with $\nu \in \{1, \ldots, 10\}$ for $\mathbf{sFAO}_{0,1}$ (——), $\mathbf{sFAO}_{\emptyset,n}$ (——) and $\mathbf{mFAO}_{0,n}$ (——).

output $\widehat{y}$ of $\mathbf{sFAO}_{0,1}$ (——), $\mathbf{sFAO}_{\emptyset,n}$ (——) and $\mathbf{mFAO}_{0,n}$ (——), respectively. In the second subplot, the respective estimation errors $e_y = y - \widehat{y}$ are plotted. Due to the choice of the poles, the estimation error of the $\mathbf{mFAO}_{0,n}$ decays

TABLE 2. System Parameters of all Estimation Methods for the Experiments

Samp. time	T_s	$100\,\mu\mathrm{s}$		
Est. meth.		$\mathbf{mFAO}_{0,n}$	$\mathbf{sFAO}_{0,1}$	$\mathbf{sFAO}_{\emptyset,n}$
Order	n	$1, 10$	1	$1, 10$
Gains	$\boldsymbol{l}$	Eq. (9)	$(0.26,\ 1.28,\ 0)^\top$	$\sqrt{2}\boldsymbol{c}$ [23]
Des. poles	$p_0^\star, p_\nu^\star$	$-2, -2+\jmath\nu$	—	—
Initial v.	$\widehat{\boldsymbol{x}}(0)$	$\mathbf{0}_3, \mathbf{0}_{21}$	$\mathbf{0}_3$	$\mathbf{0}_2, \mathbf{0}_{20}$
FLL		mFLL	sFLL	sFLL
Gain	Γ	$56\frac{1}{\mathrm{s}}$	$40\frac{1}{\mathrm{s}}$	$46\frac{1}{\mathrm{s}}$
Threshold	ε	$10^{-2}\mathrm{V}^2$	$10^{-2}\mathrm{V}^2$	$10^{-2}\mathrm{V}^2$
AWU	ω_max	$2\pi 61\ \mathrm{rad\,s^{-1}}$	—	—
	ω_min	$2\pi 49\ \mathrm{rad\,s^{-1}}$	—	—
RL	$\dot{\omega}_\mathrm{max}$	$2\pi 10^5\ \mathrm{rad\,s^{-2}}$	—	—
	$\dot{\omega}_\mathrm{min}$	$-2\pi 10^5\ \mathrm{rad\,s^{-2}}$	—	—
Initial value	$\widehat{\omega}(0)$	$2\pi 40\ \mathrm{rad\,s^{-1}}$	$2\pi 40\ \mathrm{rad\,s^{-1}}$	$2\pi 40\ \mathrm{rad\,s^{-1}}$
Filters		LPF (each)	—	—
Cut-off f.	ω_c	$2\pi 100\ \mathrm{rad\,s^{-1}}$	—	—
Initial v.	$\xi(0)$	0	—	—

significantly faster, while the overshoots in the estimation error are almost identical for all three methods (the blue line covers the orange and grey lines). Estimation is accomplished within a few milliseconds. In contrast to that, the $\mathbf{sFAO}_{0,1}$ needs about 40–50 ms to achieve an accurate estimation and the $\mathbf{sFAO}_{\emptyset,n}$ is not capable of estimating the input at all in view of the dc-offset present in the input signal.

Note that, in view of the length of the BNC cable connecting amplifier and dSPACE system, the cable acts as a high-pass filter with rather large time constant such that any dc-offset jump is damped and decays slowly within the considered time intervals. Nevertheless, note that $\mathbf{sFAO}_{0,1}$ and $\mathbf{mFAO}_{0,n}$ can track this decaying dc-offset asymptotically. The minor oscillations in all estimation responses are due to the fixed sampling frequency which yields a time lag between y and $\widehat{y}$ resulting in these oscillations (it could be decreased by reducing the sampling time).

To compare the individual estimation performances of the three estimation methods, Fig. 7 shows the dc-offset error $e_0 := y_0 - \widehat{y}_0$ and the fundamental estimation error $e_1 := y_1 - \widehat{y}_1$ which contribute equally to the overall estimation error $e_y := y - \widehat{y} = e_0 + e_1$. Since the $\mathbf{sFAO}_{\emptyset,n}$ is not capable of detecting the dc-offset, the respective e_0 signal is *not* shown in the first subplot. However, it is still capable of estimating the fundamental signal properly. In conclusion, the $\mathbf{mFAO}_{0,n}$ has the best estimation performance overall due to its simple and fast tuning capability.

B. DISCUSSION OF SCENARIO (S2)

Scenario (S2) considers a signal with ten harmonics (including fundamental) plus dc-offset. It has a *known* fundamental frequency and undergoes step-like signal parameter changes in dc-offset, harmonic amplitudes and phase angles (see above). $\mathbf{mFAO}_{0,n}$ and $\mathbf{sFAO}_{\emptyset,n}$ are now implemented with *ten* mSOGIs and sSOGIs (i.e. $n = 10$), respectively. The $\mathbf{sFAO}_{0,1}$ still comes with only *one* sSOGI. For all methods, the FLLs are turned *off* (as in Scenario (S1)), since the frequency is assumed to be known (i.e. $\widehat{f} = f$).

The results for this scenario are illustrated in Fig. 8 where the individual subplots show input y (- - -), its estimate $\widehat{y}$ and estimation error $e_y = y - \widehat{y}$ of $\mathbf{sFAO}_{0,1}$ (——), $\mathbf{sFAO}_{\emptyset,n}$ (——) and $\mathbf{mFAO}_{0,n}$ (——), respectively. Due to the parallelization of the mSOGIs, the $\mathbf{mFAO}_{0,n}$ is capable of tracking the input within a few milliseconds whereas the $\mathbf{sFAO}_{\emptyset,n}$ with parallelized sSOGIs exhibits a non-zero estimation error resulting from the missing dc-offset estimation. Note that, again, the overshoots of all estimation methods are similar (again the blue lines covers the other lines). Since the $\mathbf{sFAO}_{0,1}$ contains only one sSOGI, it is *not* capable of estimating the input signal correctly. In view of the harmonic content, the error resulting from the sampling issue is significantly higher for all estimation methods.

Fig. 9 shows the individual estimation errors e_0, e_1, …, e_{10} of dc-offset and harmonics estimation. Note that $\mathbf{sFAO}_{0,1}$ detects the dc-offset precisely; whereas the fundamental error component is affected by all other harmonic estimation errors as those are *not* estimated at all. As for Scenario (S1), the $\mathbf{sFAO}_{\emptyset,n}$ estimates the harmonic content correctly but, clearly, the dc-offset estimation is missing. The $\mathbf{mFAO}_{0,n}$ again provides the best estimation performance concerning estimation speed and accuracy – overall and in each individual signal component, respectively.

C. DISCUSSION OF SCENARIO (S3)

For Scenario (S3), the considered signal contains a dc-offset and a fundamental component. It now comes with a *varying* and *unknown* angular frequency. The signal undergoes step-like changes in frequency, phase angle and amplitude; in particular, note the interval $(0.36,\ 0.48\,\mathrm{s}]$ with zero fundamental component. For all three estimation methods, the FLLs are now activated to achieve frequency adaption as well.

In Fig. 10, input y (- - -) and its respective estimates $\widehat{y}$ of $\mathbf{sFAO}_{0,1}$ (——), $\mathbf{sFAO}_{\emptyset,n}$ (——) and $\mathbf{mFAO}_{0,n}$ (——) are shown in the first subplot. The second and third subplot show estimation error e_y, frequency f & its estimate $\widehat{f}$ of all three methods, respectively. All estimation errors e_y are only slightly affected by the frequency adaptions in the FLLs; especially the settling times do not differ too much from those of Scenario (S1). The speeds of the frequency adaption by sFLL and mFLL are almost identical with 60 ms. However, due to the dc-offset, the $\mathbf{sFAO}_{\emptyset,n}$ without the capability of dc-offset detection fails to estimate the frequency correctly (oscillations around the correct frequency occur). At $t = 0.24\,\mathrm{s}$, when the amplitude sag of -75% occurs, the mFLL of the $\mathbf{mFAO}_{0,n}$ does not overshoot like the sFLLs of $\mathbf{sFAO}_{0,1}$ and $\mathbf{sFAO}_{\emptyset,n}$. During the interval $0.36\,\mathrm{s} \leq t < 0.48\,\mathrm{s}$, when there is no ac component in y, the input signal does *not* contain any frequency information anymore (which is visualized by a missing reference). Hence, all frequency estimators try to track a non-existing reference.

For **sFAO**$_{0,1}$ (——) and **sFAO**$_{\emptyset,n}$ (——) with sFLL, this leads to frequency estimations tending to zero, where the sFLLs are locked and cannot recover even if the fundamental signal comes back within the interval $0.48\,\text{s} \leq t < 0.60\,\text{s}$. Due to AW, the frequency estimate of the mFLL is held within the predefined frequency interval $[\omega_{\min},\ \omega_{\max}]$ and does *not* tend to zero. When the ac component is present again, the mFLL is able to recover and to track the frequency correctly.

In Fig. 11, the individual estimation errors e_0 and e_1 for Scenario (S3) are shown. It can be seen that, also for this case when the FLLs are turned on, the proposed **mFAO**$_{0,n}$ (——) is the fastest method overall and for each individual signal component.

D. DISCUSSION OF SCENARIO (S4)

For Scenario (S4), a signal consisting of fundamental, nine harmonics and dc-offset is considered. It has a varying (angular) fundamental frequency and jumps in frequency, harmonic phase angles and amplitudes. Again, for all three methods, the FLLs are turned on.

Fig. 12 depicts input y (- - -) and its respective estimates $\widehat{y}$ of **sFAO**$_{0,1}$ (——), **sFAO**$_{\emptyset,n}$ (——) and **mFAO**$_{0,n}$ (——) in the first subplot and the respective estimation errors e_y in the second subplot (with identical color code). In the third subplot, actual frequency f and its estimates $\widehat{f}$ are plotted. Again, the settling times of the input estimation errors are not significantly influenced by the FLLs. But, since the **sFAO**$_{0,1}$ (——) is not designed to estimate harmonics, it fails to estimate the input accurately and ripples in e_y occur. Similar results with large ripples in e_y are obtained by the **sFAO**$_{\emptyset,n}$ (——). Moreover, both methods are not able to estimate the frequency correctly until $t \leq 0.36\,\text{s}$ (oscillations are present); after $t > 0.36\,\text{s}$, both sFLLs fail completely and are not able to recover when the fundamental ac component with frequency information comes back (similar malfunctioning as already observed in Scenario (S3)). In contrast to those, the estimation performance of the **mFAO**$_{0,n}$ (——) is still accurate within the interval $t \in [0.36\,\text{s}, 0.48\,\text{s})$ and very good for the remaining time intervals. A similar good performance of the **mFAO**$_{0,n}$ (——) can be observed in Fig. 13 for the individual dc-offset e_0 and harmonic estimation errors $e_1, \ldots, e_{10}$. Nevertheless, noise sensitivity of the **mFAO**$_{0,n}$ is rather obvious but less than that of **sFAO**$_{0,1}$ (——) and **sFAO**$_{\emptyset,n}$ (——), which both are *not* capable of achieving an accurate estimation (see e_0 & e_1 of **sFAO**$_{0,1}$ (——) and e_1,..., e_{10} of **sFAO**$_{\emptyset,n}$ (——) in particular after $t \geq 0.36\,\text{s}$).

V. CONCLUSION

A Frequency Adaptive Observer (FAO) – consisting of DC-intergrator (DCI) and parallelized modified Second-Order Generalized Integrators (mSOGIs) and a modified Frequency-Locked Loop (mFLL) with Gain Normalization (GN), sign-correct Anti-Windup (AW) decision function, Rate Limitation (RL) and Low-Pass Filters (LPFs) – has been proposed. It constitutes a unified method to estimate dc-offset, fundamental and harmonic components and (angular) frequency of arbitrarily distorted single-phase signals in grids with dc-offset. Hereby, the recently reported mSOGIs which allow for a (theoretically and) arbitrarily fast tuning of the individual harmonic estimations were used. The key observation for the design of the FAO was the observability property of the underlying signal generation system (internal model) which led to a simple and analytical tuning rule for the proposed observer by pole placement. The fast and accurate estimation performance of the proposed FAO with and without mFLL was shown by extensive measurement results which were compared to available estimation methods in literature. In future contributions, the following five main goals shall be achieved: (i) Estimation of arbitrary harmonic content without knowing the explicit harmonic orders, (ii) improvement of the frequency adaption to achieve significantly faster estimation speeds, (iii) application of the proposed FAO to three-phase systems to extract symmetrical components of all harmonic components (i.e. to extend the results in [25]), (iv) implementation on less powerful real-time systems (e.g. Arduino or Rasperry Pi) and (v) use of the FAO in closed-loop operation (e.g. in the feedback loop of power/current/voltage control).

ACKNOWLEDGMENT

The authors are deeply indebted to Prof. Dr.-Ing. Simon Schramm (Munich University of Applied Sciences) for having the chance to use the Spitzenberger-Spies amplifier and the sensor box.

REFERENCES

[1] K. R. Patil and H. H. Patel, "Modified dual second-order generalised integrator FLL for synchronization of a distributed generator to a weak grid," in *Proc. IEEE 16th Int. Conf. Environ. Electr. Eng. (EEEIC)*, pp. 1–5, Jun. 2016, doi: 10.1109/EEEIC.2016.7555824.

[2] G. Fedele, A. Ferrise, and D. Frascino, "Structural properties of the SOGI system for parameters estimation of a biased sinusoid," in *Proc. 9th Int. Conf. Environ. Electric. Eng.*, pp. 438–441, May. 2010, doi: 10.1109/EEEIC.2010.5490432.

[3] G. Zhu, Q. Yuan, and X. Yang, "Research and analysis of SOGI-QSG integral saturation in the application of grid synchronization," in *Proc. IEEE Int. Conf. Mechatronics Autom. (ICMA)*, pp. 1167–1171, Aug. 2019, doi: 10.1109/ICMA.2019.8816463.

[4] L. Hadjidemetriou, E. Kyriakides, and F. Blaabjerg, "A robust synchronization to enhance the power quality of renewable energy systems," *IEEE Trans. Ind. Electron.*, vol. 62, no. 8, pp. 4858–4868, Aug. 2015.

[5] L. Hadjidemetriou, E. Kyriakides, and F. Blaabjerg, "An adaptive tuning mechanism for phase-locked loop algorithms for faster time performance of interconnected renewable energy sources," *IEEE Trans. Ind. Appl.*, vol. 51, no. 2, pp. 1792–1804, Mar. 2015.

[6] D. Janik, J. Talla, T. Komrska, and Z. Peroutka, "Optimalization of SOGI PLL for single-phase converter control systems: Second order generalized integrator (SOGI)," in *Proc. Int. Conf. Appl. Electron.*, Sep. 2013, pp. 1–4.

[7] C. M. Hackl and M. Landerer, "Modified second-order generalized integrators with modified frequency locked loop for fast harmonics estimation of distorted single-phase signals," *IEEE Trans. Power Electron.*, vol. 35, no. 3. Mar. 2020.

[8] S. Golestan, J. M. Guerrero, J. C. Vasquez, A. M. Abusorrah, and Y. Al-Turki, "Modeling, tuning, and performance comparison of second-order-generalized-integrator-based FLLs," *IEEE Trans. Power Electron.*, vol. 33, no. 12, pp. 10 229–10 239, Dec. 2018.

[9] J. S. Park, D. C. Lee, and T. L. Van, "Advanced single-phase SOGI-FLL using self-tuning gain based on fuzzy logic," in *Proc. IEEE ECCE Asia Downunder*, Jun. 2013, pp. 1282–1288.

[10] A. E. Karkevandi and M. J. Daryani, "Frequency estimation with anti-windup to improve SOGI filter transient response to voltage sags," in *Proc. 6th Int. Istanb. Smart Grids Cities Cong. Fair (ICSG)*, Apr. 2018, pp. 188–192.
[11] T. D. C. Busarello, K. Zeb, A. Peres, V. S. R. V. Oruganti, and M. G. Simoes, "Designing a second order generalized integrator digital phase locked loop based on a frequency response approach," in *Proc. IEEE PES Innovative Smart Grid Technol. Conf. - Latin Amer. (ISGT Latin Amer.)*, Sep. 2019, pp. 1–6, doi: 10.1109/ISGT-LA.2019.8895304.
[12] C. Xie, K. Li, J. Zou, K. Zhou, and J. M. Guerrero, "Multiple second-order generalized integrators based comb filter for fast selective harmonic extraction," in *Proc. IEEE Appl. Power Electron. Conf. Expos. (APEC)*, pp. 2427–2432, Mar. 2019.
[13] Z. Xin, Z. Qin, M. Lu, P. C. Loh, and F. Blaabjerg, "A new second-order generalized integrator based quadrature signal generator with enhanced performance," in *Proc. IEEE Energy Convers. Congr. Expos. (ECCE)*, pp. 1–7, Sep. 2016.
[14] M. Mojiri, M. Karimi-Ghartemani, and A. Bakhshai, "Time-domain signal analysis using adaptive notch filter," *IEEE Trans. Signal Process.*, vol. 55, no. 1, pp. 85–93, Jan. 2007.
[15] K. De Brabandere *et al.*, "Design and operation of a phase-locked loop with Kalman estimator-based filter for single-phase applications," in *Proc. IECON 32nd Ann. Conf. IEEE Ind. Electron.*, pp. 525–530, 2006.
[16] P. Rodriguez, A. Luna, I. Etxeberria, J. R. Hermoso, and R. Teodorescu, "Multiple second order generalized integrators for harmonic synchronization of power converters," in *Proc. IEEE Energy Convers. Congr. Expos.*, pp. 2239–2246, 2009.
[17] M. R. Krstić, S. Lubura, S. Lale, M. Šoja, M. Ikić, and D. Milovanović, "Analysis of discretization methods applied on DC-SOGI block as part of SRF-PLL structure," in *Proc. Int. Symp. Ind. Electron. (INDEL)*, Nov. 2016, pp. 1–5.
[18] B. Hoepfner and R. Vick, "Symmetrical components detection with FFDSOGI-PLL under distorted grid conditions," in *Proc. Int. Conf. Smart Energy Systems and Technologies (SEST)*, pp. 1–6, Sep. 2019, doi: 10.1109/SEST.2019.8849000.
[19] F. Xiao, L. Dong, L. Li, and X. Liao, "A frequency-fixed SOGI-based PLL for single-phase grid-connected converters," *IEEE Tran. Power Electron.*, vol. 32, no. 3, pp. 1713–1719, Mar. 2017, doi: 10.1109/TPEL.2016.2606623.
[20] X. He, H. Geng, and G. Yang, "Reinvestigation of single-phase FLLs," *IEEE Access*, vol. 7, pp. 13 178–13 188, 2019.
[21] S. Golestan, J. M. Guerrero, F. Musavi, and J. Vasquez, "Single-phase frequency-locked loops: A comprehensive review," *IEEE Trans. Power Electron.*, vol. 34, no. 12, pp. 11791–11812, Dec. 2019.
[22] K. De Brabandere, "Voltage and frequency droop control in low voltage grids by distributed generators with inverter front-end," Ph.D. dissertation, Dept. Elect. Eng., Katholieke University Leuven, 2006.
[23] P. Rodriguez, A. Luna, I. Candela, R. Mujal, R. Teodorescu, and F. Blaabjerg, "Multiresonant frequency-locked loop for grid synchronization of power converters under distorted grid conditions," *IEEE Trans. Ind. Electron.*, vol. 58, no. 1, pp. 127–138, Jan. 2011.
[24] F. Muzi and M. Barbati, "A real-time harmonic monitoring aimed at improving smart grid power quality," in *Proc. IEEE Int. Conf. Smart Meas. Future Grids (SMFG)*, Nov. 2011, pp. 95–100.
[25] C. M. Hackl and M. Landerer, "A unified method for online detection of phase variables and symmetrical components of unbalanced three-phase systems with harmonic distortion," *Energies*, vol. 12, no. 17, 2019. [Online]. Available: https://www.mdpi.com/1996-1073/12/17/3243, doi: 10.3390/en12173243.
[26] Z. Dai, W. Lin, and H. Lin, "Estimation of single-phase grid voltage parameters with zero steady-state error," *IEEE Trans. Power Electron.*, vol. 31, no. 5, pp. 3867–3879, May. 2016.
[27] M. Karimi-Ghartemani, S. A. Khajehoddin, P. K. Jain, A. Bakhshai, and M. Mojiri, "Addressing DC component in PLL and notch filter algorithms," *IEEE Trans. Power Electron.*, vol. 27, no. 1, pp. 78–86, Jan. 2012.
[28] M. Xie, H. Wen, C. Zhu, and Y. Yang, "Dc offset rejection improvement in single-phase SOGI-PLL algorithms: Methods review and experimental evaluation," *IEEE Access*, vol. 5, pp. 12 810–12 819, 2017.
[29] Z. Yan, H. He, J. Li, M. Su, and C. Zhang, "Double fundamental frequency PLL with second order generalized integrator under unbalanced grid voltages," in *Proc. Int. Power Electron. Appl. Conf. Expo.*, pp. 108–113, Nov. 2014.
[30] H. K. Yada and M. S. R. Murthy, "An improved control algorithm for DSTATCOM based on single-phase SOGI-PLL under varying load conditions and adverse grid conditions," in *Proc. IEEE Int. Conf. Power Electron., Drives Energy Syst. (PEDES)*, Dec. 2016, pp. 1–6.
[31] T. Ngo, Q. Nguyen, and S. Santoso, "Improving performance of single-phase SOGI-FLL under DC-offset voltage condition," in *Proc. IECON 2014-40th Ann. Conf. IEEE Ind. Electron. Soc.*, Oct. 2014, pp. 1537–1541.
[32] H. Yi, X. Wang, F. Blaabjerg, and F. Zhuo, "Impedance analysis of SOGI-FLL-based grid synchronization," *IEEE Trans. Power Electronics*, vol. 32, no. 10, pp. 7409–7413, Oct. 2017.
[33] J. Matas, H. Martin, J. de la Hoz, A. Abusorrah, Y. A. Al-Turki, and M. Al-Hindawi, "A family of gradient descent grid frequency estimators for the SOGI filter," *IEEE Trans. Power Electron.*, 2017.
[34] R. Teodorescu, M. Liserre, and P. Rodriguez, *Grid Converters for Photovoltaic and Wind Power Systems*. Chichester, U.K.: Wiley, 2011, Early Access.
[35] W. M. Wonham, *Linear Multivariable Control: A Geometric Approach*, 3rd ed., ser. Applications of Mathematics, no. 10. Berlin, Germany: Springer-Verlag, 1985.
[36] C. M. Hackl and M. Landerer, "Modified second-order generalized integrators with modified frequency locked loop for fast harmonics estimation of distorted single-phase signals (LONG VERSION)," Feb. 2019, *arXiv:1902.04653*.

CHRISTOPH M. HACKL (Senior Member, IEEE) was born in 1977 in Mannheim, Germany. He received the B.Sc., Dipl.-Ing., and Dr.-Ing. (Ph.D.) degrees in Electrical Engineering from Technical University of Munich (TUM), in 2003, 2004, and 2012, respectively. After studying Electrical Engineering (with focus on controls and mechatronics) at Technical University of Munich (TUM), Germany and University of Wisconsin-Madison, USA. In 2018, he became a Professor for Electrical Machines and Drives, and the Head of the "Laboratory for Mechatronic and Renewable Energy Systems (LMRES)" and, in 2019, the Co-Head of the newly founded "Research Institute for Sustainable Energy Systems (ISES)" at the Munich University of Applied Sciences (MUAS), Germany. His research interests include nonlinear, adaptive and optimal control of electrical, mechatronic, and renewable energy systems.

MARKUS LANDERER was born in 1988 in Ebersberg, Germany. He received the B.Sc. and M.Sc. degrees in Electrical Engineering (with focus on controls and energy transmission/energy systems) from the Technical University of Munich (TUM), Germany, in 2013 and 2016, respectively. At the moment, he is pursuing the Ph.D. degree in Electrical Engineering with TUM. From 2016 to 2018, he was Research Associate within the research group "Control of Renewable Energy Systems" (CRES) at TUM; since 2019, he is a Research Associate within "Laboratory for Mechatronic and Renewable Energy Systems" (LMRES) at the Munich University of Applied Sciences, Munich, Germany. His research interests include nonlinear and adaptive control and modeling of electrical and renewable energy systems.